International Journal of Mass Spectrometry 287 (2009) 105–113

Contents lists available at ScienceDirect

International Journal of Mass Spectrometry

journal homepage: www.elsevier.com/locate/ijms

Influence of cluster size and ion activation method on the dissociation of cesium iodide clusters

Asiri S. Galhena[1], Christopher M. Jones[2], Vicki H. Wysocki*

Department of Chemistry, Department of Biochemistry and Molecular Biophysics, University of Arizona, Tucson, AZ 85721-0041, –>United States

ARTICLE INFO

Article history:
Received 16 December 2008
Received in revised form 10 March 2009
Accepted 15 March 2009
Available online 6 April 2009

Keywords:
Cluster
Cesium iodide
Magic number
Surface-induced dissociation (SID)
Collision-induced dissociation (CID)

ABSTRACT

Cesium iodide clusters (CsI) are simple ionic structures that are composed of different combinations of the same two atoms, cesium and iodine. When these clusters are generated by electrospray ionization, mass spectrometry analysis shows the generation of a broad m/z distribution with one or two residual cesium ions as the charge carrier(s). The formation of larger cluster assemblies was ion source dependent, and significantly influenced by source pressure. The gas-phase dissociation of these clusters was studied by collision-induced dissociation (CID) and surface-induced dissociation (SID) in a quadrupole time-of-flight mass spectrometer. SID was found to deposit more internal energy into these clusters, providing access to alternative, high energy dissociation pathways. The most significant differences were observed for larger cluster systems. Doubly charged clusters were observed to dissociate via one or two pathways, a mass stripping process and a charge splitting process. While SID yielded both fragmentation pathways, CID only accessed the mass stripping pathway.

1. Introduction

Clusters are an important group of structures as they span the chemical and physical gap between discrete atoms or molecules and solid materials, and provide clues to the transitions between the condensed and gaseous states of matter [1]. One of the keys to bridging this gap is to understand the size-dependent behavior exhibited by cluster systems. The structure, stability, energetics, and chemical properties of clusters all depend on the extent of their aggregation. While small clusters differ significantly from bulk matter, owing largely to their high surface-to-volume ratio and electronic structure, clusters of substantial size can begin to adopt bulk-like behavior. For example, clusters of CsCl and CsI form six-fold coordinated face-centered cubic (fcc) lattices despite the fact that the bulk material exists in an eight-fold coordinated body-centered cubic (bcc) lattice structure [2]. Only after the crystal exceeds some critical size will a transition to the bcc lattice structure occur [3]. Investigation of size-related phenomena in these systems may improve our understanding of several physical/chemical processes including phase transition phenomena, crystal growth, chemical catalysis, and thin film formation [4,5].

From an experimental point of view, clusters are relatively easy to form, and their ionic bonding character has allowed the development of simple models that permit different cluster configurations to be studied. Many analytical techniques and theoretical methods have been employed in cluster research [6–8]. Although all of these methods and techniques provide a significant amount of information on cluster systems, mass spectrometry stands out as a major experimental technique that offers advantages for studying size-dependent cluster properties with inherently high sensitivity. In general, most mass spectrometric analyses of clusters have been performed with electrospray ionization (ESI) [9–11], plasma desorption [12,13], laser ablation/vaporization [2,14,15], particle sputtering [16] and secondary ion mass spectrometry [17]. ESI is a gentle ionization method that has proven to be particularly useful in studying gas phase clusters. Hao et al. reported the influence of several experimental conditions such as concentration, solution pH and instrument operating conditions, including desolvation temperature, solution flow-rate, capillary voltage, cone voltage, on the formation of cluster ions [18,19] by ESI. Zhou and Wang et al. used clusters to probe the mechanism of electrospray ion formation [20,21]. Furthermore electrosprayed clusters are widely used as calibration standards for mass spectrometers.

Among the different types of cluster systems, alkali halide clusters have been most widely studied by mass spectrometry, especially singly charged positive clusters. The general formula for these clusters can be given as $(MX)_nM^+$ [22–25], where M and X

* Corresponding author at: 1306 E. University Blvd., Department of Chemistry, Box 210041, University of Arizona, Tucson, AZ 85721-0041, United States.
Tel.: +1 520 621 2628; fax: +1 520 621 8407.
E-mail address: vwysocki@email.arizona.edu (V.H. Wysocki).
[1] Present address: Georgia Institute of Technology, 901 Atlantic Drive NW, Atlanta, GA 30332, United States.
[2] Present address: Baxter Healthcare Corporation, 25212 W. Illinois Route 120, Round Lake, IL 60073, United States.

1387-3806/$ – see front matter © 2009 Published by Elsevier B.V.
doi:10.1016/j.ijms.2009.03.009

represent the cation and anion of the molecule, respectively. An important discovery in cluster science has been the identification of magic number clusters, specific combinations of M and X present in high abundance due to their extraordinary stability [23,26–29]; these magic number clusters have been attributed to the formation of cubic-like crystal structures [30]. Systematic studies into the dissociation of salt clusters of varying size provide valuable insight into their structure and stability. While such studies have been conducted in the past [18,31–33], improvements in the mass range of tandem mass spectrometers and advancements in ion activation methods allow more extensive investigation.

In addition to improving our understanding of cluster properties themselves, the simplicity of these systems provides an ideal model for studying fundamental gas-phase processes such as collisions of ions with gaseous atoms or molecules or with surfaces. These processes have played an essential role in tandem mass spectrometry, in which the kinetic energy of the projectile ion is converted into internal energy upon collision with a gaseous target (collision-induced dissociation, CID) or surface target (surface-induced dissociation, SID), followed by unimolecular dissociation of the ion post-collision. Among the alkali halide clusters, the fragmentation behavior of cesium iodide has been extensively studied by mass analyzed ion kinetic energy spectrometry (MIKES) [24,34–36], as well as high energy collision-induced dissociation [24,37–40]. It is evident from these experimental studies that small CsI clusters dissociate via unimolecular decomposition into mass stripped products through the removal of neutral CsI moieties [34,36,37,39,41]. Whetten and coworkers [42,43] performed impact-induced dissociation (analogous to SID using graphite and silicon surface targets) studies on alkali halide clusters, with the products of dissociation generated through a single step fission process along the low energy cleavage planes of these clusters.

CsI has previously been shown to form clusters consisting of as many as 350 CsI molecules [44]. The ability to form clusters across such a broad mass range allows ion activation to be probed as a function of ion size. Furthermore, a comparative study of different ion activation methods on clusters of increasing size may not only elucidate complementary fragmentation pathways of salt clusters, but also provide insight into the interactions between the projectile ion and its collision partner(s). A better understanding of the activation process for a system composed of the same two atoms can be used to shed light on the fragmentation of other large, more complex ions. The gas-phase dissociation of many large biological systems, for example, remains poorly understood partly due to the fact that the projectile ion:collision target size ratio is significantly higher than that of more thoroughly characterized model organic ions [45]. This article presents a comparative study of dissociation of cesium iodide clusters by two ion activation methods, surface-induced and collision-induced dissociation. Several different cluster moieties, including singly and doubly charged cesium iodide clusters, are dissociated and the influence of ion activation method and cluster size on ion dissociation is discussed.

2. Experimental

2.1. Samples

Cesium iodide (99.9%) and methanol (HPLC grade) were purchased from Sigma–Aldrich (St. Louis, MO) and used without further purification. The freshly prepared samples in water:methanol (50:50) with concentrations of 20–100 mg/mL were sprayed out of a home-built nano-ESI source. The samples were first loaded into glass capillaries pulled in-house (Sutter Instruments, P-97 micro-pipette puller) to a final tip diameter of 1–5 μm. A platinum wire was inserted into the glass capillary and a voltage of 1.5–2.0 kV was applied to the analyte solution. The cone voltage was varied between 50 and 150 V until optimum ion transmission was obtained. No heating or desolvation gas was used with nano-ESI.

2.2. Instrumentation

Experiments were performed in a home-modified Q-ToF II mass spectrometer (Micromass/Waters, Manchester) that has been described previously [46]. Briefly, an in-line SID device was installed in between the quadrupole mass analyzer and hexapole collision cell to allow direct comparisons of CID and SID on the same instrument. The SID device, which includes a surface holder, ion beam deflectors, and focusing lenses, is approximately 45 mm in length, with the surface holder positioned in parallel, but 8 mm above, the center of the ion beam. A shortened, 13 cm collision cell provided by Waters Corporation replaced the traditional 18.5 cm collision cell to accommodate the SID device. This allowed the conventional ion optics to remain in place, and facilitated the use of higher gas pressures within the collision cell while maintaining appropriate pressure in the adjacent ToF region. The instrument was operated in one of two modes; one that allows ion transmission through the SID apparatus without hitting the surface for single-stage MS and CID experiments, or alternatively, surface collision mode in which ions are deflected into the surface for SID experiments. This allowed direct comparison between the two ion activation methods under otherwise identical instrument conditions and similar observation time frames.

In CID mode, the experiments were performed using argon (Ar) as the collision target. The pressure was measured in the quadrupole analyzer chamber and typically maintained between 1×10^{-4} and 6×10^{-4} mbar (the actual pressure in the collision cell is different from the quadrupole chamber pressure because there is no pressure gauge connected directly to the collision cell). For SID experiments, fluorinated self-assembled monolayer (FSAM) surfaces were used as the collision target. These surfaces have previously been shown to provide efficient translational-to-vibrational energy transfer to the projectile. For SID experiments, the collision cell was operated without Ar gas with the collision cell serving solely as a hexapole ion guide. The collision voltage for the CID mode was controlled by adjusting the DC offset of the source hexapole between 0 and 200 V, relative to the collision cell (grounded). For SID, the collision voltage was varied between 0 and 190 V by setting the DC offset (10–200 V) of the source hexapole with respect to the surface voltage (~10–20 V). The actual collision voltage was calculated by subtracting the difference between these two voltages. All collision energies are listed as the product of the voltage difference times the precursor ion charge state.

2.3. Self-assembled monolayer (SAM) surfaces

Glass surfaces (18 mm × 12 mm) coated with a 10-Å layer of titanium followed by a 1000-Å layer of gold (Evaporated Metal films Corp., Ithaca, NY) were used as substrates for the SID collision targets. The Au-coated glass slide was first UV cleaned for 15 min, rinsed with ethanol, and immersed in a 1 mM ethanolic solution of 2-(perfluorodecyl) ethanethiol for 24 h. Following this step the surface was immersed in reagent grade ethanol and sonicated for 5 min in an ultrasonic bath. Sonication was repeated two more times with fresh ethanol solutions. Finally the glass surfaces, coated with a fluorinated SAM, were air-dried and attached to the surface holder of the SID setup. The surface preparation technique is further explained elsewhere [47,48]. The 2-(perfluorodecyl) ethanethiol used for SAM surfaces was synthesized by the Chemical Synthesis Facility of the Department of Chemistry, University of Arizona.

3. Results and discussion

3.1. Generation and characterization of CsI clusters by electrospray ionization

One of the important strategies for generating and transmitting cluster ions is to have fine control over the instrument operation conditions. The distributions of salt cluster ions were found to be influenced markedly by the magnitude of cone voltage, source temperature, ESI solvent and source pressure. Higher source pressures are critical for observing high mass cluster ions. Fig. 1 shows the nano-ESI mass spectrum of 15 mg/mL CsI solution sprayed out of 50:50 methanol:water. Two different charge distributions of clusters are evident in the mass spectrum. One belongs to the singly charged ion series and the second one to the doubly charged series. The singly charged cluster ions have the generic formula of $(MX)_nM^+$ and each of the peaks in this series are separated by a mass of 259.8 Da, corresponding to a molecular weight of one CsI moiety. The second series corresponds to doubly charged CsI and has the formula of $(MX)_qM_2^{2+}$. Each peak corresponding to a cluster with an even number of Cs atoms overlaps with a singly charged ion, while peaks corresponding to an odd number of Cs atoms appear in between the singly charged cluster peaks (i.e., $(CsI)_2Cs_2^{2+}$ and $(CsI)_4Cs_2^{2+}$ will overlap in m/z with $(CsI)_1Cs^+$ and $(CsI)_2Cs^+$ respectively, whereas $(CsI)_3Cs_2^{2+}$ will correspond solely to the doubly charged ion). One significant difference between the two series is that the doubly charged ions always appear to be lower in intensity than the singly charged moieties. Such an effect can be attributed to two causes: first, the doubly charged ion series with an even number of Cs perfectly overlaps with the singly charged series, so the total ion intensity of these peaks is the sum of the contributions from the singly charged ion and the overlapping doubly charged ion. Second, some authors suggest that the additional charge on the doubly charged clusters may induce instability into the crystal structures, resulting in their lower abundance [49,50].

A predominant feature in the MS spectra of these cluster systems is the uneven intensity distribution of the singly charged ion series. As marked in Fig. 1, the high abundance of certain singly charged ions is attributed to the formation of magic number clusters. There are two forms of magic number clusters. One corresponds to the arrangement of atoms in a symmetric fashion, i.e., a cubic $3 \times 3 \times 3$ structure, a tetragonal $3 \times 3 \times 5$ structure, an orthorhombic $3 \times 5 \times 7$ structure, etc. (the term "cubic-like" has been used to collectively describe these structures) [16,29]. The second corresponds to surface terraces built upon completed cubic lattices [51,52]. For example, if three rows of three CsI molecules in the cluster of $3 \times 5 \times 7$ are removed, an abundant, $n = 43$ cluster is formed (Fig. 1). Although these structures are pseudo-cubic, they have been shown to be considerably stable [2].

Another interesting feature in the spectrum is the onset of the doubly charged cluster series. This effect is the so-called "critical size" effect [26], and defined as the smallest possible cluster size that can be formed with multiple charges. In our experiments, the smallest doubly charged cluster observed corresponds to $q = 21$. This property is found to be dependent on several experimental conditions such as capillary voltage, and desolvation temperature [53], but a detailed experimental study of this property was not the subject of this research.

3.2. Collision- and surface-induced dissociation of small $(CsI)_nCs^+$ clusters

In order to probe the influence of cluster size on dissociation patterns, a small cluster system, $(CsI)_6Cs^+$ was selected in the quadrupole analyzer and fragmented either by SID or multiple-collision CID. The repetitive units of Cs and I that comprise these clusters, facilitate the interpretation of their dissociation pathways because the major fragmentation products must be any combination of just two atoms. Furthermore, because these small clusters have relatively low masses, the internal energy required to initiate fragmentation should also be low, thus a subtle change in the collision energy may reflect a significant difference in dissociation pathways.

Fig. 2 shows the CID and SID comparison spectra of $(CsI)_6Cs^+$ at collision energies of 10 eV (Fig. 2a and c, respectively) and 20 eV (Fig. 2b and d, respectively). The spectra are shown at identical laboratory collision energies for comparison, although the amount of internal energy deposited is also a function of the collision target. For SID experiments, an FSAM surface was chosen as the collision target due to its favorable energy transfer properties. Translational to vibrational energy transfer in SID is known to vary with surface properties such as stiffness, terminal group mass, and packing of the SAM film. The energy transfer efficiency for FSAMs has been reported between 20 and 28%, among the highest reported for SAM

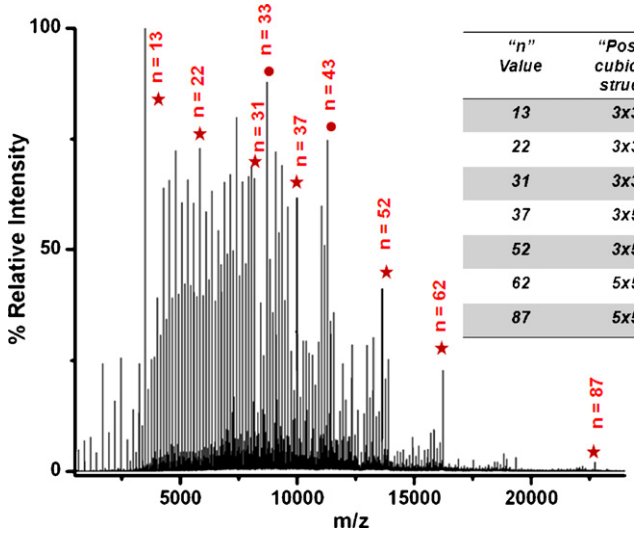

"n" Value	"Possible cubic like" structure	# of atoms
13	3x3x3	27
22	3x3x5	45
31	3x3x7	63
37	3x5x5	75
52	3x5x7	105
62	5x5x5	125
87	5x5x7	175

Fig. 1. Mass spectrum of 15 mg/mL CsI solution under positive nano-ESI conditions in a Q-ToF mass spectrometer. The spectrum is composed of both singly and doubly charged cluster ions in the range of 250–26,000 m/z. Evidence for stable "cubic-like" structures are evident at $n = 13$, 22, 31, 37, 52 and 62. The table in the inset represents one possible symmetric structure for each magic number cluster. (⋆) Cubic-like clusters

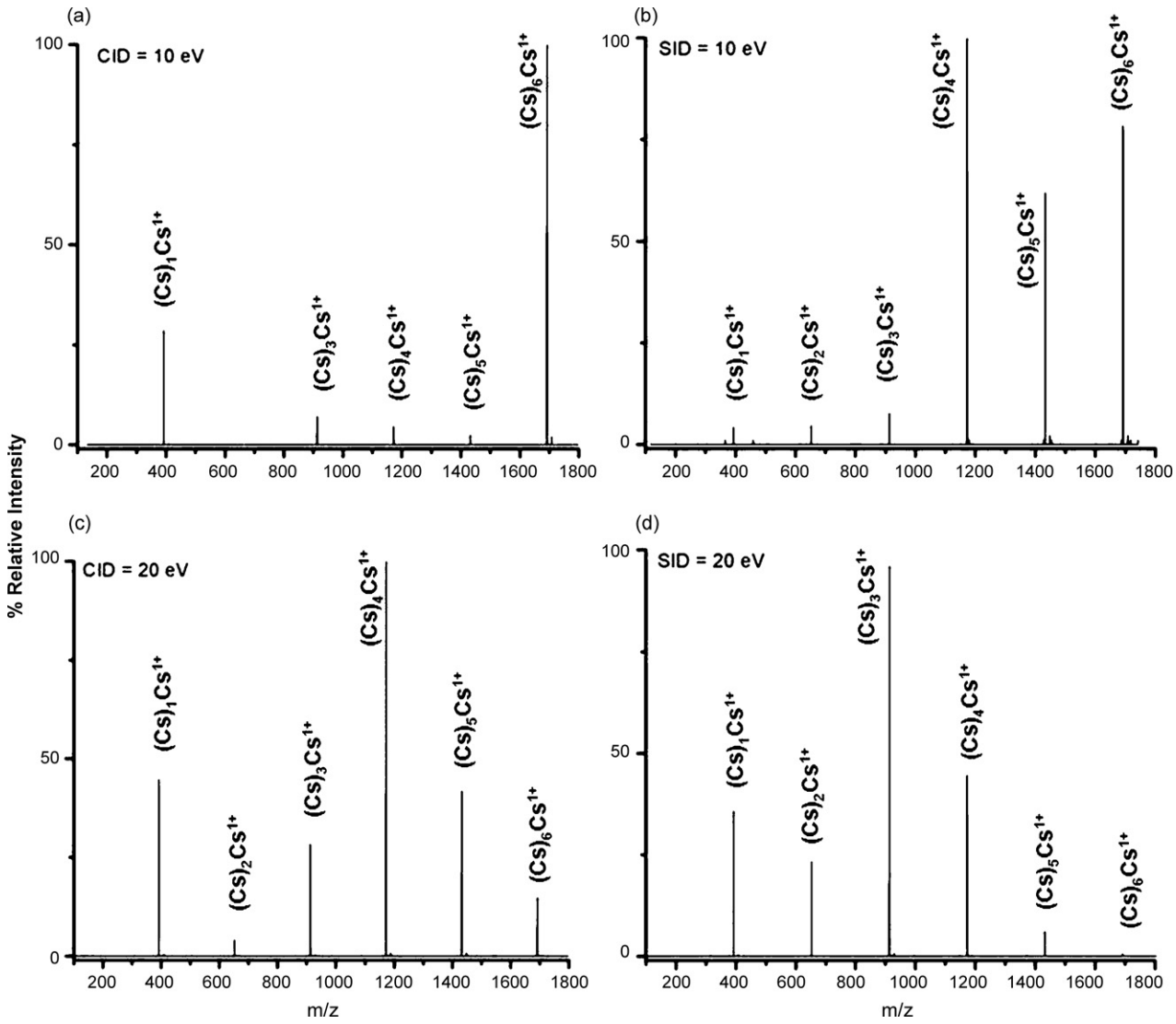

Fig. 2. CID and SID spectra of $(CsI)_6Cs^+$ clusters in the Q-ToF instrument; (a and b) CID spectra at collision energies of 10 and 20 eV; (c and d) SID spectra at collision energy energies of 10 and 20 eV respectively.

films. Energy transfer in CID varies with the mass of the target gas and the number of collisions. Here, argon was chosen as the collision gas. In general both CID and SID spectra show extensive fragmentation of the molecular ion to generate a series of singly charged fragment ions. The fragment ions have the same empirical formulas as the precursor ion, $(CsI)_nCs^+$. Because the precursor ion carries only a single charge, the formation of such singly charged fragments has to come from the loss of neutral CsI moieties [35,36]. The most striking difference between the two ion activation methods is the fragmentation efficiency. For example, at a collision energy of 20 eV (Fig. 2d), SID shows almost no precursor ion survival while the precursor remains at ~20% relative abundance by CID (Fig. 2b).

One other notable difference is the appearance of the $(CsI)_2Cs^+$ cluster fragment (m/z = 652) in the SID spectra (Fig. 2c and d). This fragment is absent from the 10 eV CID spectrum (Fig. 2a) and only present in low abundance at 20 eV CID (Fig. 2b). Previous collision-induced dissociation studies of the same alkali-halide system by Drewello and coworkers [54], also revealed a similar dissociation pattern for $(CsI)_6Cs^+$. They observed a significant reduction in the $(CsI)_2Cs^+$ cluster formation, not only for $(CsI)_6Cs^+$, but for a number of other small CsI clusters as well. Russell and coworkers [55] found the n = 2 cluster to exhibit the lowest stability and the lowest abundance when they fragmented cesium iodide clusters (n = 0–7) by ion mobility-CID-MS. Even by increasing the CID collision energy (data not shown) this fragment is negligible, indicating that the low-energy, stepwise nature of CID likely causes $(CsI)_6Cs^+$ to dissociate through another channel(s) prior to gaining enough energy to produce $(CsI)_2Cs^+$. However, SID, by providing higher energy in single step, allows alternative/additional dissociation pathways, such as the formation of $(CsI)_2Cs^+$. This interpretation is further supported by the breakdown curves for the n = 6 cluster (Fig. 3). In the CID energy-resolved MS/MS (ERMS) breakdown curve, the relative abundance of the n = 2 cluster fragment is never greater than 5% over the range of collision energies from 10 to 40 eV (Fig. 3a). With SID, at a collision energy of 10 eV, the relative abundance of the same cluster fragment is calculated as ~8% and increases up to ~28% at a collision energy of 40 eV (Fig. 3b). Other substantial evidence for different internal energy deposition by SID is provided by the relative abundance of the precursor ion at each collision energy. At a collision energy of 10 eV, CID shows ~70% precursor ion retention, whereas SID shows only ~30%. At the same time, the SID ERMS curves for the fragment clusters are also shifted to lower energy thresholds, indicating the ability of SID to deposit higher amounts of internal energy at comparable lab-frame energies. Although SID

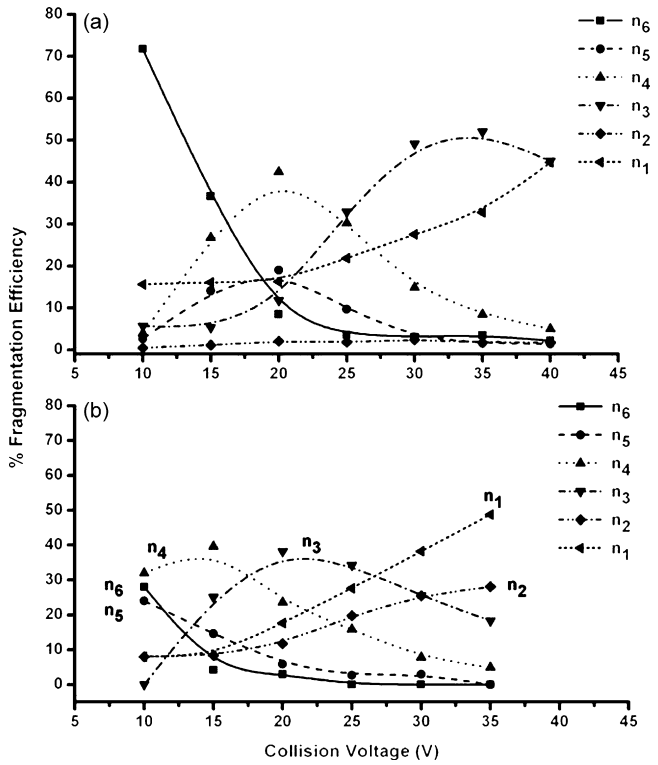

Fig. 3. Energy-resolved MS/MS graphs of $(CsI)_6Cs^+$ clusters activated by (a) CID, analyzer pressure 8×10^{-5} mbar (b) SID, analyzer pressure 1×10^{-5} mbar. The different ion intensities were integrated and plotted in relative abundance to the total ion intensity. The series of points generated for each fragment ion was fit with the most appropriate sigmoidal or exponential fitting.

provides additional internal energy, there is no substantial evidence that the excess energy afforded by SID leads to a difference in the fundamental mechanism of cluster fragmentation (other than the formation of the $(CsI)_2Cs^+$ fragment). This could be due to the fact that these clusters are sufficiently small that both activation methods readily provide enough energy to access similar dissociation channels.

Despite the differences noted, CID and SID of small CsI clusters are largely similar, with both activation methods predominantly causing a sequential loss of neutral CsI molecules. The production of a singly charged $(CsI)_1Cs^+$ ion from the original $n = 6$ cluster, however, appears to compete with the neutral CsI stripping pathway, and is significant even at low collision energies, especially when the complex is dissociated by CID (Scheme 1). For example, at 10 eV

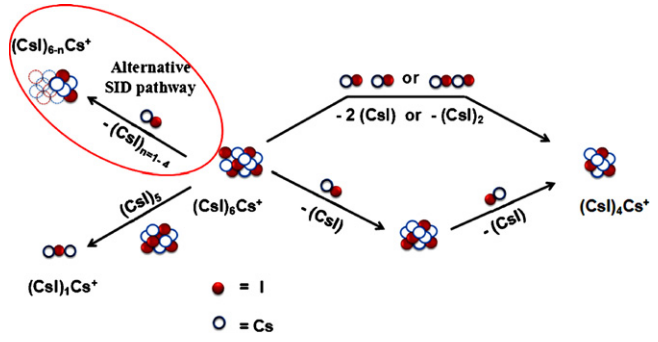

Scheme 1. Dissociation channels observed for the fragmentation of $(CsI)_6Cs^+$ clusters. CID leads solely to consecutive losses of neutral monomers or dimers of CsI as well as charged $(CsI)Cs^+$. SID provides additional dissociation pathways by losing larger size n(CsI) moieties. Structures are not represented by the most stable conformer.

CID collision energy (Fig. 2b), the $(CsI)_1Cs^+$ fragment is over 25% in relative abundance, while the $n = 3$ and $n = 4$ fragments are less than 10%. Because the $n = 3$ and $n = 4$ fragments result from sequential CsI losses [35,36] and increase in abundance at even higher energies, the fact that $(CsI)_1Cs^+$ is observed at lower energy means it is most likely the result of a direct fragmentation from the precursor ion (Scheme 1). A third dissociation pathway, the loss of two neutral CsI units, is also possible by CID. As shown in the breakdown graph, $(CsI)_6Cs^+$ dissociates into $(CsI)_5Cs^+$ by loss of a single CsI moiety. It concurrently dissociates into $(CsI)_4Cs^+$ by the net loss of two CsI units, as evident from the co-appearance of both $(CsI)_5Cs^+$ and $(CsI)_4Cs^+$ clusters at similar collision energies in the breakdown graph. However, under the current instrument observation time frame, it is difficult to conclude that the formation of $(CsI)_4Cs^+$ is solely from a loss of a neutral CsI dimer, not from a sequential loss of two neutral CsI monomers. Judging from the breakdown graph, the loss of multiple units of neutral CsI moieties ($n = 2, 3, 4$, Scheme 1) by SID seems plausible, but again, it is difficult to distinguish this from multiple sequential losses of single CsI moieties.

3.3. SID and CID comparison of singly and doubly charged medium and large size clusters

Most studies performed to date on larger salt clusters have been performed by using CID. SID, however, is known to rapidly deposit higher internal energies into projectile ions and is believed to be particularly beneficial in the fragmentation of more massive projectile ions such as multiply charged protein complexes [45,56]. This section is mainly focused on comparing the dissociation of mid-size salt clusters with one and/or two charges, activated by CID or SID.

Fig. 4 shows CID and SID comparisons for the $(CsI)_{30}Cs^+$ cluster at three different collision energies. Although it was originally assumed that the selected precursor ion was a singly charged ion, the inset of Fig. 4a shows a series of fragment ions separated by $\Delta m/z = 130$ Da, clearly indicating that the singly charged precursor ion was contaminated with the overlapping doubly charged $(CsI)_{60}Cs_2^{2+}$ cluster. To prevent any confusion, the collision energies for this cluster system are presented as collision voltages (without correcting for the charge state). The SID and CID spectra are strikingly different for this medium size cluster. The most prominent difference is the amount of dissociation, where SID shows far more extensive fragmentation. The SID spectrum acquired at a collision potential of 30 V shows (Fig. 4d) fragment ions corresponding to the singly charge cluster series at both the high and low mass ends of the spectrum. Generation of high m/z fragments comes solely from the overlapped doubly charged precursor ions. With increasing collision voltage (Fig. 4e and f), SID generates mostly small size fragment clusters, indicating higher internal energy conversion and secondary fragmentation of large clusters that remain unfragmented at V = 30. In contrast, at collision energies even higher than those used to generate the SID spectra, CID shows a reduced amount of fragmentation (Fig. 4a–c). At a collision potential of 70 V, the fragment ions show a Gaussian like distribution centered at m/z equivalent to $(CsI)_{26}Cs^+/(CsI)_{52}Cs_2^{2+}$, whereas at 90 V the fragment ion distribution is shifted to a lower m/z, centered at $(CsI)_{47}Cs_2^{2+}$. The fragmentation channel(s) observed by CID can again be interpreted as the sequential loss of neutral CsI units (a mass stripping process). SID fragment ions, on the other hand, are generated by both the mass stripping process and a mass splitting process, where the precursor cluster divides into two complementary fragments of various sizes, both of which retain the charge.

Because the singly charged clusters for which "n" is an even number have the potential of overlapping with doubly charged cluster ions "$2n$", a doubly charged cluster with an odd number of CsI moieties was selected to simplify interpretation of the MS/MS spectra. For this comparison, $(CsI)_{43}Cs_2^{2+}$ was selected and frag-

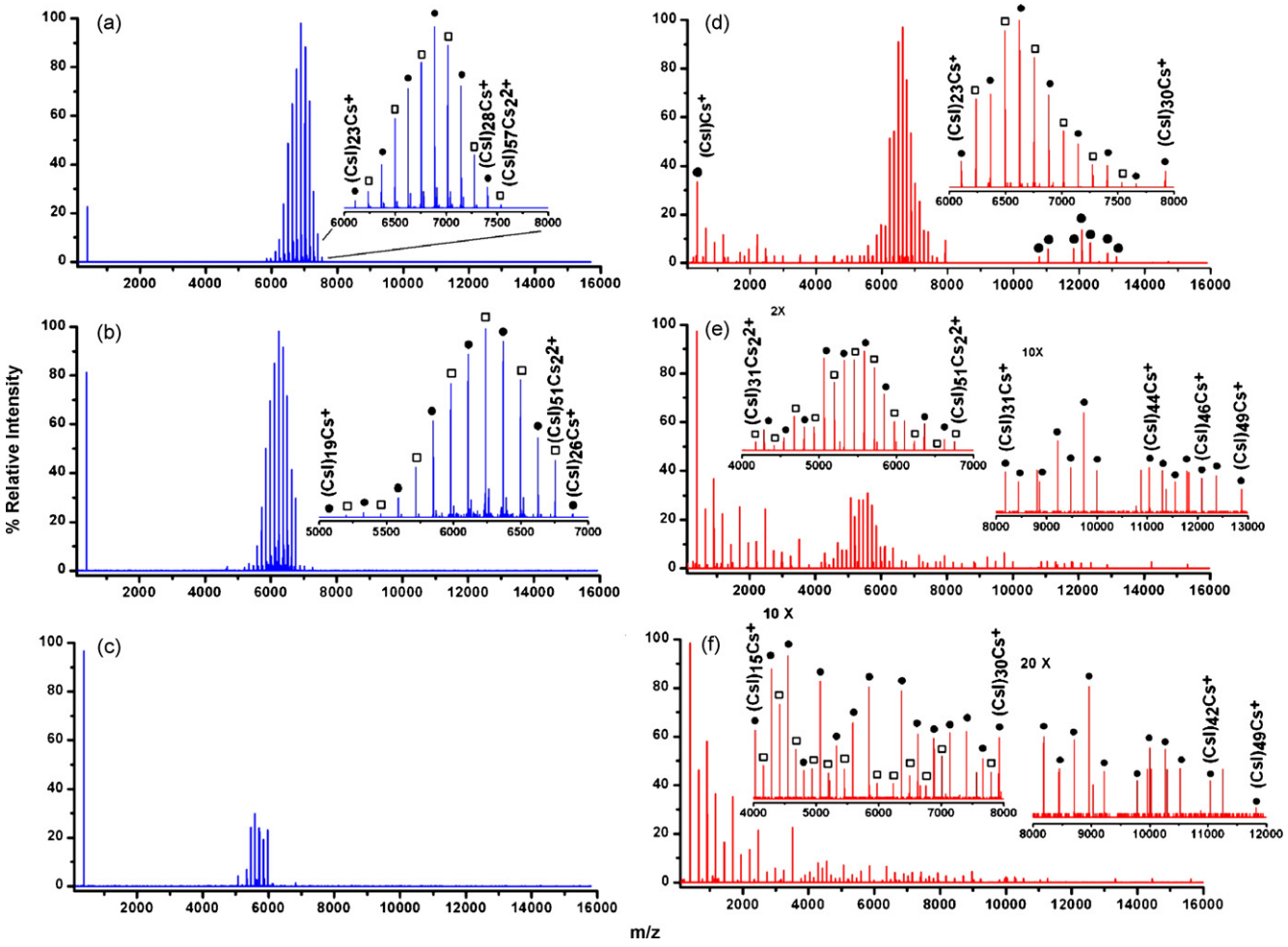

Fig. 4. Comparison of CID (left panel) and SID (right panel) spectra of $(CsI)_{n=30}Cs^+/(CsI)_{q=60}Cs_2{}^{2+}$. CID spectra were collected at collision voltages of (a) 70 V, (b) 90 V, and (c) 110 V, respectively. SID spectra were collected at collision voltages of (d) 30 V, (e) 50 V, and (f) 70 V, respectively. Insets are blowups of different m/z regions of CID and SID. (●) Singly charged cesium iodide cluster fragments; (□) doubly charged cesium iodide cluster fragments.

mented. $(CsI)_{43}Cs_2{}^{2+}$ has a nominal mass of 11434.3 Da. The MS spectrum in Fig. 1 shows the formation of stable doubly charged clusters, including $(CsI)_{43}Cs_2{}^{2+}$. Presumably, the formal charges are separated to minimize inter-charge repulsions. Previous research on salt clusters hypothesized that multiply charged cluster ions would readily adopt a conformer with a regular flat surface and thicknesses of a single molecule [18]. Although we are not certain of the $(CsI)_{43}Cs_2{}^{2+}$ cluster structure, an elongated conformation could provide added stability by separating the two charges at opposite sides of the cluster. As shown in Fig. 5, the SID and CID spectra of $(CsI)_{43}Cs_2{}^{2+}$ are again remarkably different. By CID the $(CsI)_{43}Cs_2{}^{2+}$ cluster still fragments predominantly through the loss of neutral CsI units to produce doubly charged fragments from the doubly charged precursor (Fig. 5a and b). Although CID shows neutral CsI loss as the dominant fragmentation pathway, a second fragmentation pathway involving production of singly charged $(CsI)_1Cs^+$ was also evident. In contrast with the CID results, SID shows an alternative charge separation/mass splitting process, producing singly charged fragments from a doubly charged precursor ion (Fig. 5c and d). The charge separation, or fission process and the neutral loss process are two competing pathways, with the probability of each dependent upon energy availability and cluster size. With CID, the neutral loss process is dominant as it is driven by the limited internal energy available from collision with Ar.

The fission process produced by SID can be explained with the help of the two-body interaction theory [3,57]. The formation of a doubly charged cluster is a product of a fusion process (fusion of two singly charged clusters). As one would expect there is a long-range Coulombic repulsive force between two singly charged clusters moieties. However, as the two multi-atom ions are brought within chemical bonding distance, the cluster should transform from an unstable to a kinetically stable (or metastable) cluster [58]. With increasing inter-charge distance, the Coulombic repulsion becomes less and the doubly charged ion becomes more stable. Martin calculated the lowest possible energy configurations for several doubly charged NaI clusters and showed a clear trend in which cluster stability increases with the cluster size. In other words, the energy barrier preventing the most stable configuration from undergoing Coulombic dissociation increases as the size of the cluster increases [58]. Upon activation, if the added excess energy is sufficient to overcome this energy barrier, the cluster would undergo a reverse reaction, a fission process, producing charge separated products. With $(CsI)_{43}Cs_2{}^{2+}$, CID does not supply enough energy to overcome the barrier for the fission process to occur. However it still provides sufficient energy to eject neutral $(CsI)_n$ units generating doubly charged mass-stripped product clusters (the doubly charged products still have enough mass to exist as stable product clusters). Previous CID studies published by Cooks and coworkers [53] on doubly charged NaI cluster systems have also revealed a similar fragmentation pattern, where high mass NaI clusters predominantly dissociated by loss of neutral NaI units and low mass clusters dissociated by charge splitting.

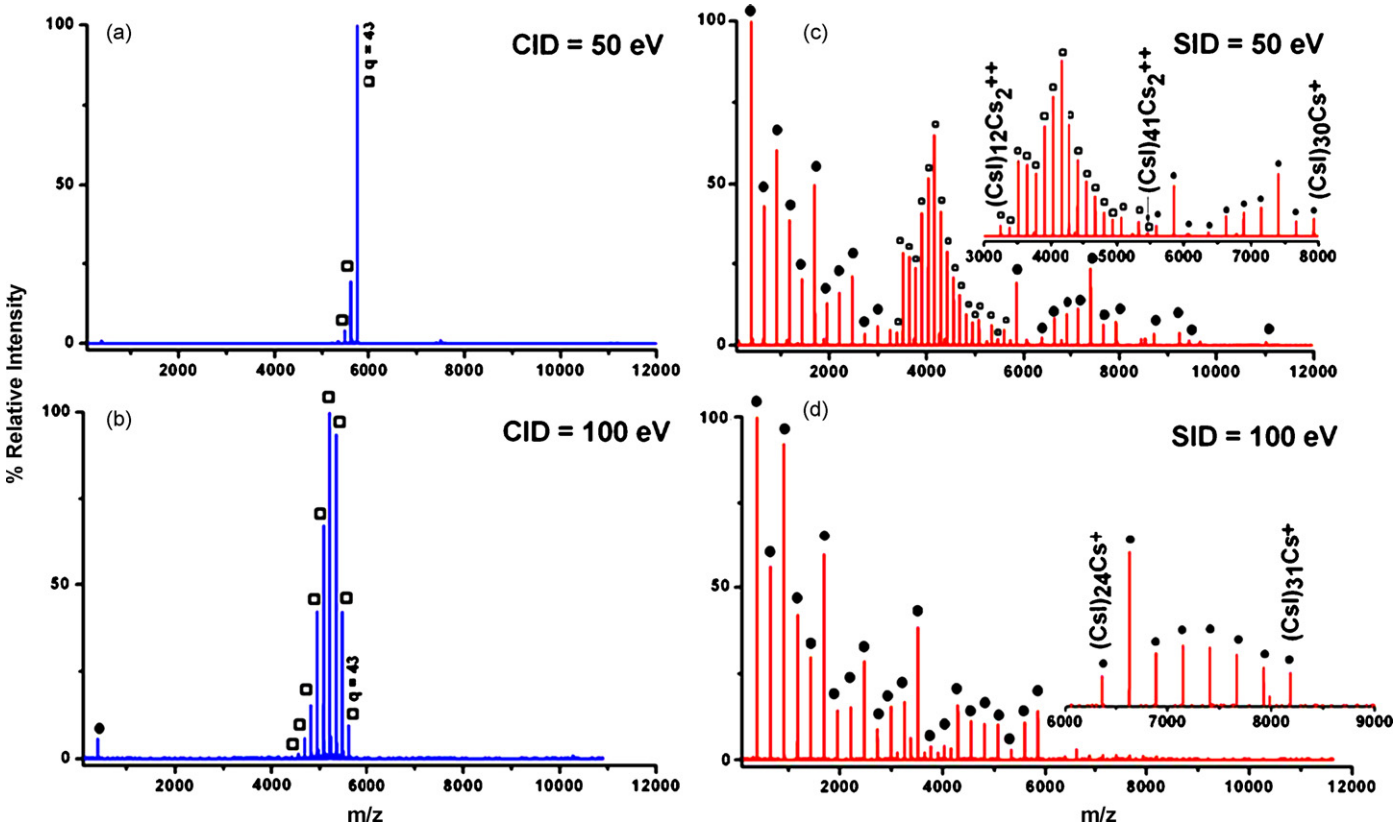

Fig. 5. Comparison of CID (left panel) and SID (right panel) spectra of the doubly charged $(CsI)_{43}Cs_2^{2+}$ cluster. Inset in SID collision energy 50 eV, shows two distinct charge distributions, doubly and singly charged. SID at collision energy of 100 eV, shows predominantly singly charged fragments. (●) Singly charged cesium iodide cluster fragments; (□) doubly charged cesium iodide cluster fragments.

For CsI experiments we propose that SID deposits higher internal energy into the projectile ion, enabling it to overcome the energy barrier for the fission process. This claim is supported by breakdown curves for small CsI clusters, in which it is evident that the dissociation onset for any given fragment ion occurs at a lower laboratory collision energy by SID relative to CID. For CID of large CsI clusters, activation even at the highest attainable collision energies is insufficient to access the fission pathways. Further supportive evidence for this observation is provided by Whetten and coworkers, in their impact-induced dissociation experiment of NaF cluster systems. They concluded the formation of charge split products has to come from a single-step fracture process not from a sequential losses of NaF [42]. The computed energy for such fragmentation as a single-step process is calculated as 3.3 eV, significantly higher energy than that of single neutral loss of a NaF moiety. Interestingly, impact-induced dissociation studies of alkali-halide systems with graphite and silicon surfaces by Whetten and coworkers [42,59,60] exhibited some differences from the current study, especially for doubly charged clusters. At lower impact energies in their instrument, the preferred fragmentation pathway was the generation of only two complementary charge split fragments. In contrast, the Q-SID/CID-ToF instrument showed more extensive fragmentation behavior, namely a distribution of charge split fragments. There could be several reasons for such a discrepancy. First, Whetten and coworkers did not examine the same projectile ions and used graphite and silicon surfaces as their impact surfaces, whereas in our experiments, fluorocarbon monolayer surfaces are used as the collision partner. Fluorinated surfaces are well characterized and known to provide higher internal energies compared to graphite and silicon, and could contribute to the extensive dissociation patterns in our experiments [48]. Another difference in the experiments is the observation time frames of the two instrument configurations. Whetten's impact-induced dissociation work is performed at the back end of a time-of-flight reflectron chamber. The observation time frame of such an instrument configuration lies in the sub-microsecond time window, allowing the detection of only products from fast fragmentation channels [61]. If the formation of fragment ions is on the order of microseconds or longer, the ions are detected as precursor ions not fragments. However, the Q-SID/CID-ToF instrument has an observation time frame of several hundred microseconds to milliseconds, allowing the detection of slower dissociation processes. This is likely a significant factor in the observation of more extensive fragmentation in our instrument configuration. At higher collision energies, the impact-induced dissociation spectra of Whetten and coworkers showed featureless fragmentation behavior (no enhancement of magic number clusters), an observation the authors attributed to the transfer of enough internal energy to transform the cluster into a molten (more liquid like) form. Such a transformation would distort the crystal structure information and would generate only arbitrary fragments. At higher SID collision energies in the Q-ToF, extensive fragmentation with an enhancement of certain fragment ions was observed. These enhancements are found to be "magic number" clusters [23,26,28,29,62], corresponding to symmetrically stable cubic-like crystal structures with lattices of $3 \times 3 \times 3, 3 \times 3 \times 5, 5 \times 5 \times 5$, etc., similar to those observed in the MS spectrum. It is not well understood why impact-induced dissociation lacked these magic number clusters, while Q-ToF SID produces more featured spectra, but the short time frame of Whetten's experiment would detect fragmentation of only the most highly excited ions. In-addition there is a difference in the energy of the ions generated from the source. In the Q-ToF instrument, nano-ESI is used and the source pressure is raised to enhance the transmission of high mass ions; this may also result in some collisional cooling

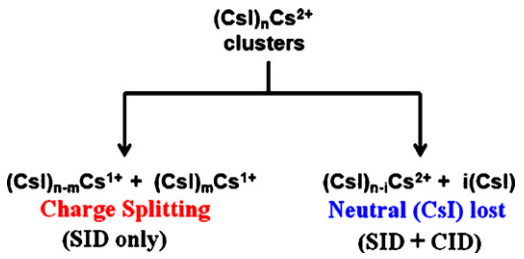

Scheme 2. Dissociation channels observed for the fragmentation of $(CsI)_qCs^{2+}$ clusters. CID leads solely to consecutive losses of neutral CsI, while access to an additional charge separation pathway is provided by SID.

or damping of the ion internal energy prior to surface collision. Activation of the thermally cooled precursor ions results in more controlled dissociation patterns. Another factor is the difference of the impact angles employed in the two experiments. With Q-ToF SID, the impact angle on the surface is presumed to be ~45°, whereas the impact angle in the ToF reflectron configuration is approximately perpendicular (~0° relative to the surface normal). With ~0° impact angles the internal energy conversion is higher, producing highly heated precursor ions upon impact and perhaps opening "shattering" mechanisms where direct dissociation at the surface occurs [63].

The SID/CID dissociation patterns observed for doubly charged clusters of $(CsI)_{43}Cs_2^{2+}$ are summarized in Scheme 2. The major fragmentation pathway for the CID process is again the sequential loss of *n*-number of (CsI) units to generate mass stripped fragment ions. The CID fragmentation data for this cluster do not provide evidence for the neutral-dimer loss route as we observed for the small size cluster systems. However the production of a singly charged cluster moiety, $(CsI)Cs^+$, is found to be a major pathway. In contrast, SID could access the same fragmentation pathways observed by CID, but also revealed alternative high energy dissociation pathways to generate charge split products. Such information is beneficial in understanding the cluster morphology and its low energy crystal structures.

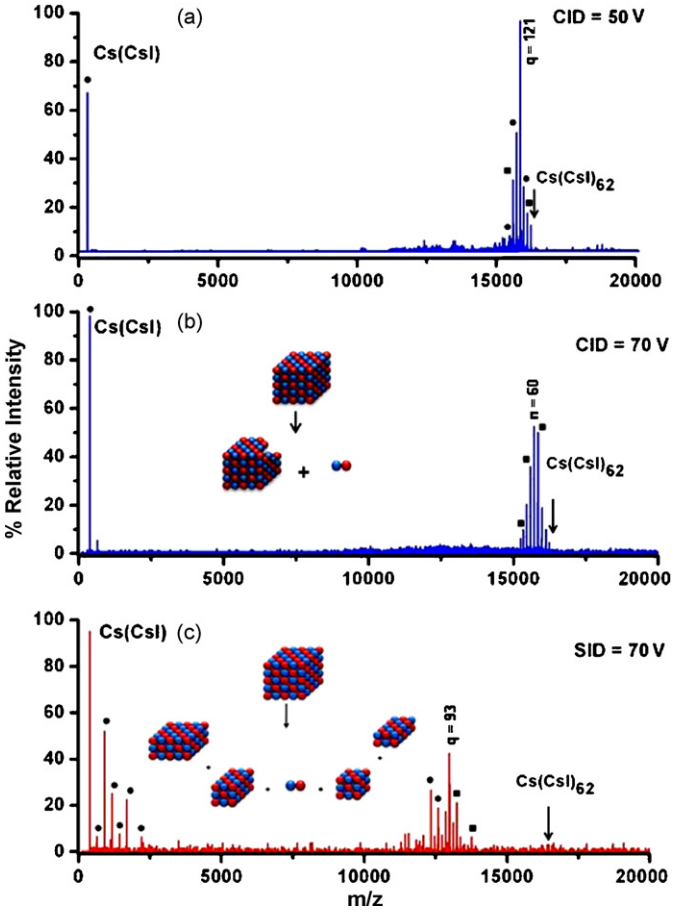

Fig. 6. MS/MS spectra of $(CsI)_{62}Cs^+/(CsI)_{124}Cs_2^{2+}$, activated by (a) CID at a collision voltage of 50 V. (b) CID at collision voltage 70 V. The inset represents the dominant fragmentation pathway which is the sequential loss of neutral (CsI) or formation of charged $(CsI)Cs^+$ with CID. (c) SID, at a collision voltage of 70 V. The inset shows the pictorial representation of the SID fragmentation process to generate many different sized clusters.

The dissociation of even larger cluster systems by CID and SID is of interest, as these systems carry larger mass per unit charge and allow further investigation into the influence of ion activation as a function of cluster size. Fig. 6 shows the SID and CID comparison spectra of $(CsI)_{62}Cs^+/(CsI)_{124}Cs_2^{2+}$, a stable cubic crystal with the lattice structure of $5 \times 5 \times 5$ and a m/z of 16241.1 Da. One of the challenges in dissociating such large cluster systems is their poor transmission and low abundance. Consequently, longer spectral acquisition times were required to overcome this problem. The fragmentation behavior was similar to the medium-sized clusters in that SID deposited higher internal energy and allowed access to both the charge split and mass stripped fragmentation pathways, whereas only the mass stripped pathway was observed by CID.

These results clearly indicate the capability of SID to access alternative high energy dissociation pathways. More importantly, we were able to fragment CsI clusters larger than those previously reported in the literature, and compare their dissociation by both CID and SID under the same instrument operating conditions.

4. Conclusions

In summary, the dissociation of CsI clusters of varying sizes has been studied by CID and SID in a Q-ToF instrument. The use of the same instrument to perform SID and CID allows a valid comparison between the two activation methods. For small size cluster systems, there are few significant differences between the two ion activation methods. The CID ERMS graph reveals the formation of mass stripped product ions by unimolecular dissociation. The same process was observed by SID, but each fragment ion appears at lower laboratory collision energy, indicative of higher internal energy deposition. For medium and large size clusters, CID could readily access the low energy neutral loss dissociation pathway to produce mass-stripped fragment clusters but not the high energy charge fission process. In contrast SID, could access both the competing mass-stripping and charge splitting pathways, offering more extensive fragmentation of the precursor ion cluster.

Acknowledgements

This work supported by National Science Foundation DBI grant CHE 024447 for the development of the Q-ToF instrument and NIH grant 5R01 GM 051387 for the experiments on fragmentation. CMJ thanks Pfizer for a Graduate Research Fellowship in Analytical Chemistry.

References

[1] A.J. Stace, J. Phys. Chem. A 106 (2002) 7993.
[2] Y.J. Twu, C.W.S. Conover, Y.A. Yang, L.A. Bloomfield, Phys. Rev. B 42 (1990) 5306.
[3] T.P. Martin, J. Chem. Phys. 69 (1978) 2036.
[4] T.D. Mark, Int. J. Mass Spectrom. Ion Process. 79 (1987) 1.
[5] A.W. Castleman, Int. J. Mass Spectrom. Ion Process. 118 (1992) 167.
[6] A.W. Castleman, R.G. Keesee, Acc. Chem. Res. 19 (1986) 413.
[7] T.P. Martin, Phys. Rev. B 15 (1977) 4071.
[8] F. Honda, G.M. Lancaster, Y. Fukuda, J.W. Rabalais, J. Chem. Phys. 69 (1978) 4931.
[9] M. Yamashita, J.B. Fenn, J. Phys. Chem. 88 (1984) 4671.
[10] M. Yamashita, J.B. Fenn, J. Phys. Chem. 88 (1984) 4451.

[11] C.M. Whitehouse, R.N. Dreyer, M. Yamashita, J.B. Fenn, Anal. Chem. 57 (1985) 675.
[12] R.D. Macfarlane, D.F. Torgerson, Science 191 (1976) 920.
[13] D.F. Torgerso, R.P. Skowrons, R.D. Macfarla, Biochem. Biophys. Res. Commun. 60 (1974) 616.
[14] V.E. Bondybey, J.H. English, J. Chem. Phys. 76 (1982) 2165.
[15] O.F. Hagena, Z. Phys. D: At. Mol. Clusters 20 (1991) 425.
[16] J.E. Campana, T.M. Barlak, R.J. Colton, J.J. Decorpo, J.R. Wyatt, B.I. Dunlap, Phys. Rev. Lett. 47 (1981) 1046.
[17] G.S. Groenewold, A.D. Appelhans, G.L. Gresham, J.C. Ingram, A.D. Shaw, Int. J. Mass Spectrom. 178 (1998) 19.
[18] C.Y. Hao, R.E. March, T.R. Croley, J.C. Smith, S.P. Rafferty, J. Mass Spectrom. 36 (2001) 79.
[19] C.Y. Hao, R.E. March, J. Mass Spectrom. 36 (2001) 509.
[20] S.L. Zhou, M. Hamburger, Rapid Commun. Mass Spectrom. 10 (1996) 797.
[21] G.D. Wang, R.B. Cole, Anal. Chem. 70 (1998) 873.
[22] K.L. Busch, R.G. Cooks, Science 218 (1982) 247.
[23] T.M. Barlak, J.R. Wyatt, R.J. Colton, J.J. Decorpo, J.E. Campana, J. Am. Chem. Soc. 104 (1982) 1212.
[24] M.A. Baldwin, C.J. Proctor, I.J. Amster, F.W. Mclafferty, Int. J. Mass Spectrom. Ion Process. 54 (1983) 97.
[25] J.E. Campana, B.N. Green, J. Am. Chem. Soc. 106 (1984) 531.
[26] O. Echt, K. Sattler, E. Recknagel, Phys. Rev. Lett. 47 (1981) 1121.
[27] O. Echt, A.R. Flotte, M. Knapp, K. Sattler, E. Recknagel, Phys. Chem. Chem. Phys. 86 (1982) 860.
[28] J. Muhlbach, K. Sattler, P. Pfau, E. Recknagel, Phys. Lett. A 87 (1982) 415.
[29] T.M. Barlak, J.E. Campana, R.J. Colton, J.J. Decorpo, J.R. Wyatt, J. Phys. Chem. 85 (1981) 3840.
[30] E.C. Honea, M.L. Homer, R.L. Whetten, Phys. Rev. B 47 (1993) 7480.
[31] M.P. Ince, B.A. Perera, M.J. Van Stipdonk, Int. J. Mass Spectrom. 207 (2001) 41.
[32] L.M. Wu, J.W. Denault, R.G. Cooks, L. Drahos, K. Vekey, J. Am. Soc. Mass Spectrom. 13 (2002) 1388.
[33] N. Mirsaleh-Kohan, S. Ard, A.A. Tuinman, R.N. Compton, P. Weis, M.M. Kappes, Chem. Phys. 329 (2006) 239.
[34] T.G. Morgan, M. Rabrenovic, F.M. Harris, J.H. Beynon, Org. Mass Spectrom. 19 (1984) 315.
[35] H.J. Hwang, D.K. Sensharma, M.A. Elsayed, J. Phys. Chem. 93 (1989) 5012.
[36] T. Drewello, R. Herzschuh, J. Stach, Z. Phys. D: At. Mol. Clusters 28 (1993) 339.
[37] P.J. Derrick, A.W. Colburn, M.M. Sheil, E. Uggerud, J. Chem. Soc. Faraday Trans. 86 (1990) 2533.
[38] C.D. Bradley, P.J. Derrick, Org. Mass Spectrom. 28 (1993) 390.
[39] K. Vekey, G. Czira, Org. Mass Spectrom. 28 (1993) 546.
[40] Y.J. Lee, M.S. Kim, J. Phys. Chem. A 101 (1997) 6148.
[41] K. Vekey, K. Ludanyi, Org. Mass Spectrom. 29 (1994) 615.
[42] R.D. Beck, P. Stjohn, M.L. Homer, R.L. Whetten, Science 253 (1991) 879.
[43] R.D. Beck, P. Stjohn, M.L. Homer, R.L. Whetten, Chem. Phys. Lett. 187 (1991) 122.
[44] F. Sobott, H. Hernandez, M.G. McCammon, M.A. Tito, C.V. Robinson, Anal. Chem. 74 (2002) 1402.
[45] V.H. Wysocki, C.M. Jones, A.S. Galhena, A.E. Blackwell, J. Am. Soc. Mass Spectrom. 19 (2008) 903.
[46] A.S. Galhena, S. Dagan, C.M. Jones, R.L. Beardsley, V.N. Wysocki, Anal. Chem. 80 (2008) 1425.
[47] T.E. Kane, A. Somogyi, V.H. Wysocki, Org. Mass Spectrom. 28 (1993) 1665.
[48] J.H. Callahan, A. Somogyi, V.H. Wysocki, Rapid Commun. Mass Spectrom. 7 (1993) 693.
[49] J. Simons, P. Skurski, R. Barrios, J. Am. Chem. Soc. 122 (2000) 11893.
[50] K. Sattler, J. Muhlbach, O. Echt, P. Pfau, E. Recknagel, Phys. Rev. Lett. 47 (1981) 160.
[51] C.W.S. Conover, Y.A. Yang, L.A. Bloomfield, Phys. Rev. B 38 (1988) 3517.
[52] J.E. Campana, B.I. Dunlap, Int. J. Mass Spectrom. Ion Process. 57 (1984) 103.
[53] D.X. Zhang, R.G. Cooks, Int. J. Mass Spectrom. 196 (2000) 667.
[54] R. Herzschuh, T. Drewello, Int. J. Mass Spectrom. 233 (2004) 355.
[55] F.A. Fernandez-Lima, C. Becker, K. Gillig, W.K. Russell, M.A.C. Nascimento, D.H. Russell, J. Phys. Chem. A 112 (2008) 11061.
[56] A.S. Galhena, S. Dagan, C.M. Jones, R.L. Beardsley, V.H. Wysocki, Anal. Chem. 80 (2008) 1425.
[57] T.P. Martin, J. Chem. Phys. 72 (1980) 3506.
[58] T.P. Martin, J. Chem. Phys. 76 (1982) 5467.
[59] P.M. Stjohn, R.D. Beck, R.L. Whetten, Z. Phys. D: At. Mol. Clusters 26 (1993) 226.
[60] R.D. Beck, P.S. John, M.L. Homer, C. Yeretzian, R.L. Whetten, Am. Chem. Soc. Abstr. 204 (1992) 264.
[61] C.M. Gamage, F.M. Fernandez, K. Kuppannan, V.H. Wysocki, Anal. Chem. 76 (2004) 5080.
[62] O. Echt, A.R. Flotte, M. Knapp, K. Sattler, E. Recknagel, Ber. Bunsen Phys. Chem. 86 (1982) 860.
[63] K. Park, K. Song, W.L. Hase, Int. J. Mass Spectrom. 265 (2007) 326.